Ultimate capacity of a curved multi-span arch bridge subjected to railway loads

C. Molins, J. Casas and P. Roca
Technical University of Catalonia (UPC), Department of Construction Engineering, Barcelona.

ABSTRACT: Railway loads are the largest that can be applied on bridges and their values have increased significantly during the twentieth century. In spite of that, few studies have been devoted to the ultimate capacity of existing curved multi-span arch bridges subjected to this type of loads. To appraise the actual behavior of these bridges, a very singular construction was selected: the Tosses viaduct in Queralbs (Catalonia), belonging to the rack railway line between Ribes de Freser and Núria in the Pyrenees. This multi-span bridge has twelve un-symmetric plain concrete arches spanning 6.10 to 8.20 m. The un-symmetry of the arches is owed to a longitudinal slope of 12%. Preliminary analysis were developed using a simple axle along the bridge. After that, Eurocode 1 railway vertical and horizontal loads had been considered. In particular, the influence of horizontal loads: braking and centrifugal forces is analyzed. Also the capacity of the intermediate abutments to independent some parts of the bridge is appraised.

1 INTRODUCTION

Curved multiarch bridges are complex structures showing specific phenomena such as lateral thrusts in piers due both dead and live loads. Railway loads are especially severe on these bridges due to their intrinsic magnitude as well as the significant side effects due to brake, starting and centrifugal forces.

In order to better understand the behaviour of curved multiarch bridges, a particular case has been selected to be studied in both the service and the ultimate conditions by means of a non-linear calculation approach. The construction chosen is the Tosses viaduct in Queralbs, built in 1930 as part of the structures belonging to the rack railway line between Ribes de Freser and Núria in the Catalonian Pyrenees.

This multi-span bridge is composed of twelve un-symmetric plain concrete arches spanning 6.10 to 8.20 m. Its plan describes a very sharp curve with radius of 80 m. The un-symmetry of the arches is owed to a longitudinal slope of 12%. The highest piers, exceeding a height of seventeen meters, are also un-symmetric. Some of them are widened to become robust abutments.

To perform the analyses, a numerical model specifically developed for the structural analysis of 3D masonry skeletal constructions –the so-called Generalized Matrix Formulation (GMF)–, was selected. This numerical model takes into account most of the phenomena involved in the strength capacity of the structure, such as cracking in tension, yielding and crushing in compression and second order equilibrium. More details about the model can be found in Molins and Roca (1998).

Only a few studies have been carried out on the load capacity of multi-span arch bridges. Among these, the studies carried out on scale models by Melbourne et al. (1995) and Prentice and Ponniah (1994) are to be mentioned. In addition, few references can be found about analysis of multi-arch bridges. The selected model, based on an extension of conventional matrix cal-

culation to masonry structures, has been successfully applied to the analysis of single and multi-arch bridges (Molins and Roca, 1998). One dimensional F.E. procedures have also been applied to multi-arch bridges (Brencich et al, 2001). None of these references deals with curved bridges which require full 3D modeling.

Preliminary analysis were developed using a simplified transverse line load along the bridge. After that, Eurocode 1 railway vertical and horizontal loads had been considered. In addition, the influence of horizontal loads (braking or starting and centrifugal forces) on the response of the bridge is analyzed.

2   TOSSES VIADUCT

2.1   Introduction

The overall length of the Tosses viaduct, including the wing-walls, is 142.6 m (Figure 1). The viaduct is organised in four groups of three arches with deep piers between them that allow a partial demolition of three arches (between deep piers) in case of war. Such design was mandatory at the time, owing to the proximity (10 km) to the border with France.

All twelve arches are plane and the curvature is provided by the piers which present trapezium shaped cross sections. From historic documents on the design we know that Séjourné expressions were used to define the section of the piers and the arches. The designer justified his final decisions on the geometry based on similar international references such as the bridges in the line Chamonix-Montenvers with a slope of 22% and a curve of 80 m of radius, or in the line Martigny-Chatelard with a slope of 7% and a curve of 60 m of radius.

2.2   Geometry

Table 1 summarizes the main geometrical properties of the bridge. The geometry of the arches was adapted to the steep slope of the platform. Figure 2a shows the definition of the geometry of the intrados of the arches spanning 8.20 m, formed by two different circular curves of different radii with centres vertically separated 1.224 m. Figure 2b shows the variable depth of the vaults.

The piers have a longitudinal slope of 1:40 and transverse slopes of 1:25 to the centre of the curve and 1:20 on the other side. The transverse slopes provided to the piers present continuity in the spandrel walls till the platform.
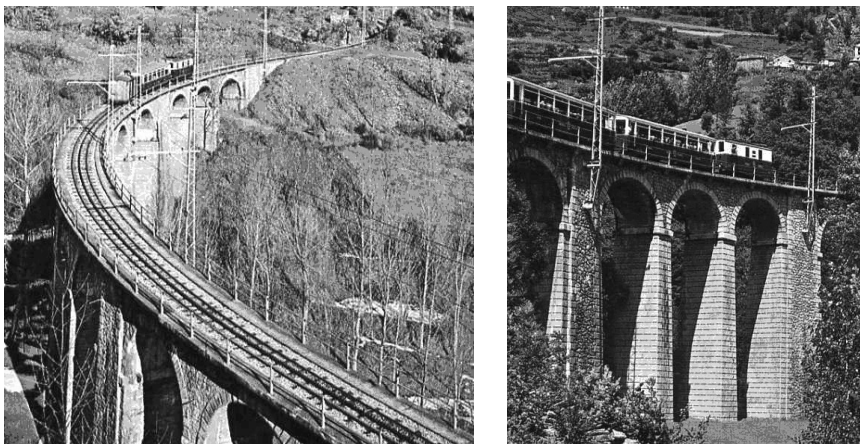
Figure 1 : Tosses Viaduct.
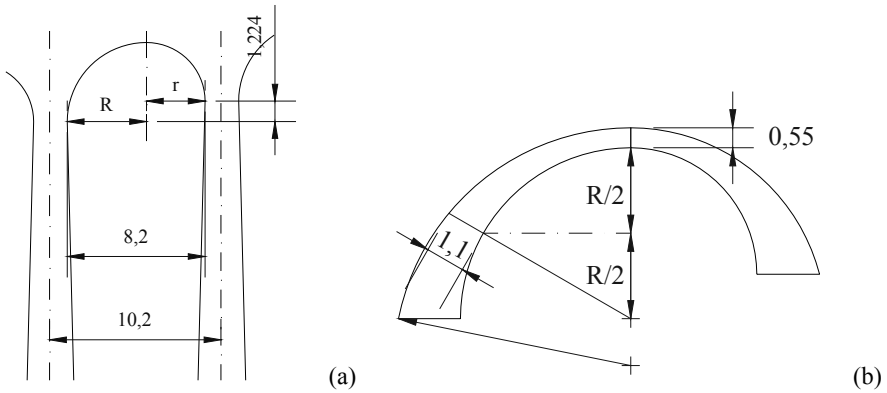
Figure 2 : (a)Definition of the intrados of the arches, and (b) definition of the depth of the vaults.

Table 1 : Main geometrical properties of the bridge.

LARGE ARCHES	
Shape	Semicircular (2 radii)
Free span	8.20 m
Arch thickness	0.55-1.10 m
Arch width	3.36 m
SMALL ARCHES	
Shape	Semicircular (2 radii)
Free span	6.10 m
Arch thickness	0.55-1.10 m
Arch width	3.36 m
OTHER GEOMETRICAL DATA	
Deep piers	4-5 m
Piers thickness (8.20 m arches)	2.00 m
Piers thickness (6.10 m arches)	1.50 m
Thickness of infill on the crown	0.70 m
Height of the tallest pier	19.60 m
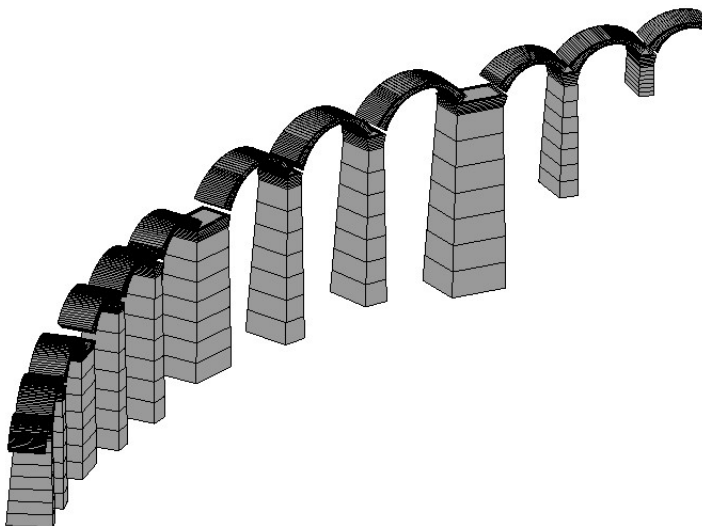
Figure 3 : Complete model of the Tosses viaduct.
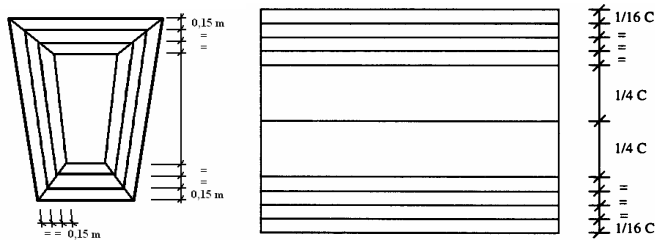
Figure 4 : Discretization of the typical trapezium shaped cross section of a pier and of an arch.

2.3 Model

The full bridge was modelled including all arches and piers (Figure 3). Each arch was modelled by eight (8) elements, four for each half of different radius, and each pier was modelled by one element. The connection between piers and the springing of the arches was modelled by rigid ends. The final model was composed of 232 nodes and 107 GMF elements. The contribution to the strength of the infill and the spandrel walls was neglected (of course, its weight was taken into account). For the definition of the piers composed partially by ashlars and by rubble masonry fifteen different quadrilateral areas were required as shown in Figure 4a. Figure 4b shows the discretization of the typical cross section of the arches with ten quadrilaterals.

2.4 Materials

The average material properties of the fabric (Table 2) were estimated based on information available on the component materials. The masonry average properties were estimated using empiric formulae such as the one provided in Eurocode 6. An ultimate strain of 0.0035 was assumed for concrete.

Table 2 : Main mechanical properties used in the analyses.

CONCRETE OF ARCHES	
Deformational modulus	20 000 N/mm^2
Compressive strength	25.0 N/mm^2
Tensile strength	0.01 N/mm^2
Unit weight	24.0 kN/m^3
MASONRY OF PIERS	
Deformational modulus	5 000 N/mm^2
Compressive strength	10.0 N/mm^2
Tensile strength	0.01 N/mm^2
Unit weight	24.0 kN/m^3

2.5 Loading

Dead loads (DL) and live loads (LL) produced by trains on the structure have been considered. LL includes the weight of trains and tangential forces due to braking and starting. In this study, conventional railway loads according to Eurocode 1 are considered in spite of the fact that the current rack loads are significantly smaller. In addition, the combined effect of railway LL and action of the wind was analyzed. The vertical loads considered were: (a) one axle along the bridge (as a reference), (b) 4 axle of 250 kN each (SET 1), according to the locomotive weight considered in Eurocode 1, (c) the latter axle plus 5 m of uniform 80 kN/m loading (SET 2), (d) the 4 axle plus 20 m of uniform 80 kN/m loading (SET 3), (d) SET 2 plus tangential starting load: 31 kN/m uniformly distributed along the train; and (f) SET 3 plus tangential starting load. The loading schemes are shown in Figure 5.

According to EC-1, centrifugal forces had to be applied at 1,80 m above the rail; their characteristic value is obtained from:

$$Q_{tk} = \frac{V^2}{127r}(f \cdot Q_{vk}) \quad q_{tk} = \frac{V^2}{127r}(f \cdot q_{vk})$$

where Q_{tk} and q_{tk} are the point or distributed centrifugal forces in kN and kN/m respectively, Q_{vk} and q_{vk} are the characteristic vertical forces: 250 kN and 80 kN/m respectively; r is the radius of the curve; V the speed in km/h (in that case only 20 km/h) and f is a coefficient valued 1.00 in this structure. Numerical values of the forces are Q_{tk} = 9.84 kN and q_{tk} = 3.15 kN/m. These loads, when compared with those produced by the action of the wind on the bridge, are a tiny fraction. Consequently, they were disregarded.
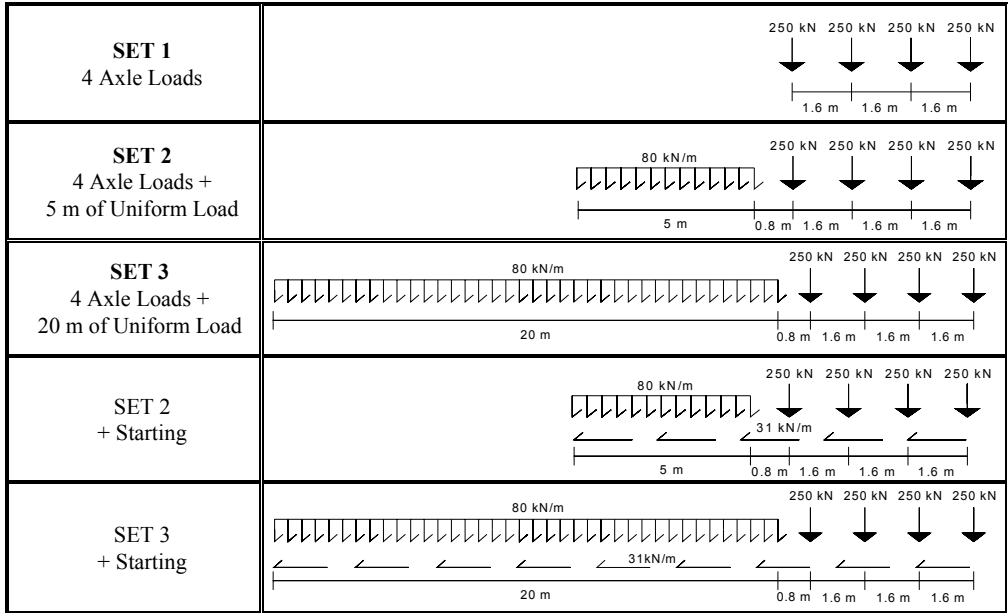
Figure 5 : Railway load patterns used in the analyses.

3 RESULTS

Arches and piers are under compression when subjected to DL and the stresses are very low. When subjected to an axle LL along the bridge, the lowest capacity was found in the arches 7th, 8th and 9th, which present the largest spans of 8.20 m while the rest of the arches span 6.10 m. Figure 6 shows the load capacity of the critical part of the bridge, the group of arches 7th to 9th, subjected to an axle load or to the SET 1 of railway loads. Table 3 provides the numerical values of the diagrams presented in Figure 6. It is worth noting that the arches 7th and 9th are influenced by the stiffness of the wide piers which independent each group of three arches. The lowest capacity under an axle load is 1.00 MN and it is achieved in the 8th arch. But minimum values in arches 7th and 9th are very close to it (1.10 MN). In all those cases, failure was obtained when concrete in the extrados of the loaded section reached its ultimate strain without completing a mechanism. To assess this result, some analyses were also made with a larger ultimate strain for concrete that presented significantly higher failure loads.

However, when subjected to SET 1 loading, owing to the spreading of the load, the minimum failure load increases to 2.50 MN (corresponding to a load factor (LF) of 2.50) and is achieved at the crown of the 9th arch. More specifically, it was obtained at 0.80 m from the crown (distance 77.04 in Table 3). In this case, failure was also determined by the ultimate strain of concrete, but it is achieved at the springing of the arch 8th close to the 9th. Figure 7 shows the stress state and the deformed shape at failure corresponding to the minimum capacity. A seven hinge

mechanism is almost formed. The hinge at the base of the pier is not fully developed but the pier is flexible enough to allow large rotations.
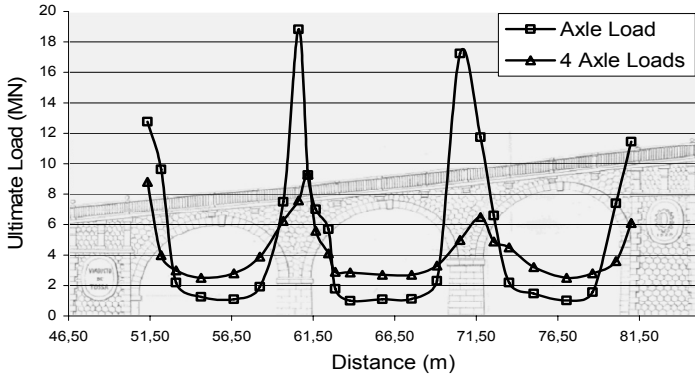
Figure 6 : Influence of the loads position on the ultimate capacity, for one axle and four axle loads.

Table 3 : Failure loads (MN).

	Distance (m)	Axle Load	4 Axle Loads
7th arch	51,35	12,75	8,80
	52,17	9,63	4,00
	53,10	2,20	3,00
	54,62	1,25	2,50
	56,64	1,10	2,80
	58,24	1,93	3,90
	59,66	7,50	6,25
	60,60	18,83	7,60
8th arch	61,18	9,25	9,30
	61,65	7,00	5,60
	62,43	5,69	4,10
	62,86	1,78	2,90
	63,77	1,00	2,85
	65,74	1,10	2,70
	67,54	1,13	2,70
	69,09	2,30	3,30
	70,51	17,25	5,00
9th arch	71,75	11,75	6,50
	72,58	6,60	4,90
	73,51	2,20	4,50
	75,02	1,48	3,20
	77,04	1,03	2,50
	78,64	1,58	2,80
	80,07	7,40	3,60
	81,01	11,45	6,10

Figure 8 shows the LF obtained using the three loading sets. The total load of each set is 1.00 MN for SET 1, 1.40 MN for SET 2 and 2.60 for SET 3. In spite of having different amounts of load, the minimum load factors for each set are almost identical and they are also very similar through the three arches (Figure 8 and Table 4). The main difference appears in the 9th arch, in which loading SETS 2 and 3 present a larger LF owing to the larger horizontal thrust that can be resisted by arches 7th and 8th which bear the favorable uniform load. This fact is particularly noticeable for SET 3. Figure 9 shows the failure mechanism for SET 3 on the crown of arch 8th.

Simultaneous action of railway weights and starting affects the minimum values of the load factors in both loadings SET 2 and SET 3. In particular, for the 9th arch. The inclusion of characteristic wind loads in combination with railway vertical loads had very little effect on the ultimate capacity of the bridge.
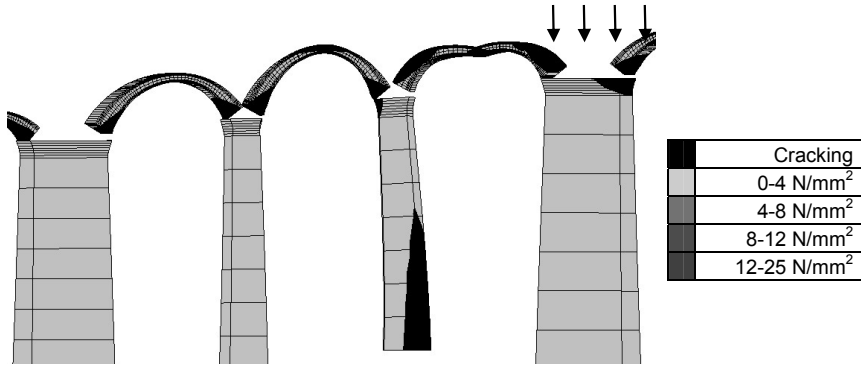
Figure 7 : Stress state and deformation (x100) of the arch subjected to a 4 axle load on the worst position.
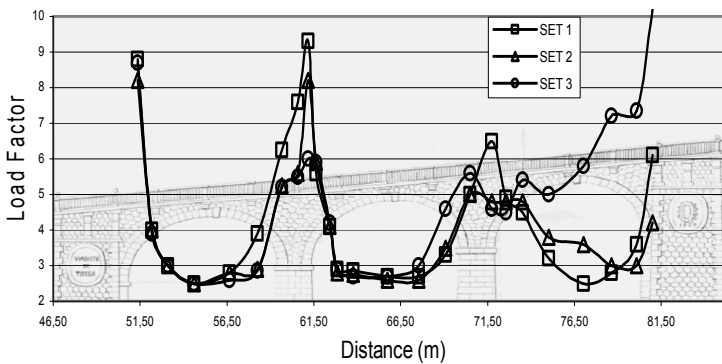
Figure 8 : Influence of the loads position on the ultimate capacity, for loading sets 1 to 3.
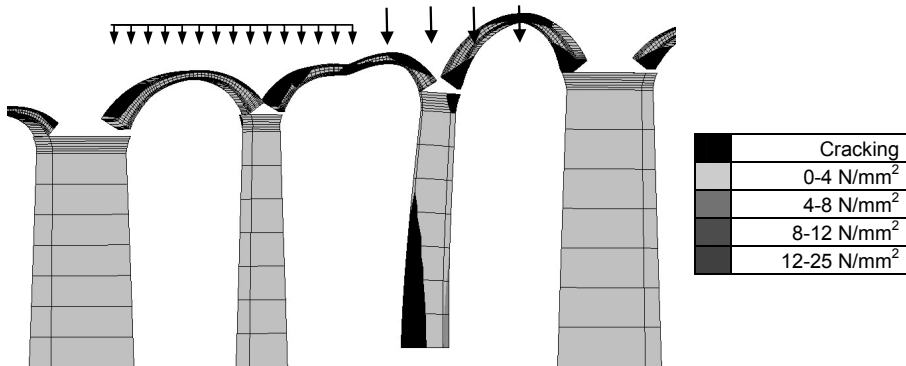
Figure 9 : Stress state and deformation (x100) of arches subjected to SET 3 loading on the crown of 8th.

4 CONCLUSIONS

The ultimate capacity of a curved multi-arch bridge subjected to design railway loads, including different patterns of live loads, starting and braking forces and wind action, has been analyzed using the GMF method. The worst loading patterns on the bridge and its critical position have been found and discussed. The ultimate loads experience significant changes when tangential forces due to starting are included. Wind action had very little influence on the ultimate capacity of the bridge.

Table 4 : Load Factors for loading sets 2 and 3, and including starting.

	Distance (m)	SET 2	SET 3	SET 2+Start	SET 3+Start
7th arch	51,35	8,20	8,70	6,00	5,30
	52,17	4,00	3,90	5,70	5,30
	53,10	3,00	3,00	3,80	3,50
	54,62	2,50	2,50	3,10	3,10
	56,64	2,80	2,60	4,00	3,30
	58,24	2,90	2,85	4,80	3,20
	59,66	5,25	5,20	6,10	3,40
	60,60	5,60	5,50	7,50	3,40
8th arch	61,18	8,20	6,00	8,30	3,70
	61,65	5,90	5,90	6,90	3,70
	62,43	4,10	4,20	6,60	3,90
	62,86	2,80	2,90	3,60	3,50
	63,77	2,75	2,70	2,90	3,50
	65,74	2,60	2,70	2,00	3,30
	67,54	2,60	3,00	1,80	4,20
	69,09	3,50	4,60	1,90	4,00
	70,51	5,00	5,60	2,40	3,80
9th arch	71,75	4,80	4,60	2,70	3,90
	72,58	4,80	4,50	2,70	3,90
	73,51	4,80	5,40	3,10	3,80
	75,02	3,80	5,00	2,20	3,50
	77,04	3,60	5,80	1,90	3,20
	78,64	3,00	7,20	1,80	2,20
	80,07	3,00	7,35	2,00	2,20
	81,01	4,20	10,00	2,80	2,70
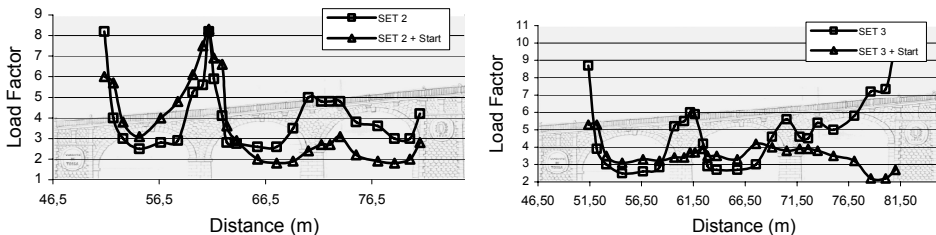
Figure 10: Influence of the load position on the ultimate capacity, for sets 2 and 3, and including starting.

ACKNOWLEDGMENTS

REFERENCES

Brencich, A. and De Francesco, U. 2004. Assessment of multispan masonry arch bridges. I: Simplified approach. *Journal of Bridge Engineering*, v 9, n 6, p 582-590.

Melbourne, C., Gilbert, M. and Wagstaff, M. 1995. The behaviour of multi-span masonry arch bridges. *Proc. 1st Int. Conference Arch Bridges*. London: Thomas Telford.

Melbourne, C. and Tao, H. 1998. The behaviour of open spandrel brickwork arch bridges. *Arch bridges, Proceedings of the 2nd international conference on arch bridges*. Rotterdam: A. A. Balkema.

Molins, C. and Roca, P. 1998. Load capacity of multi-arch masonry bridges. *Arch Bridges*. Rotterdam:A.A. Balkema.

Molins, C., Roca, P. and Pujol, A. 2001. Numerical simulation of the structural behaviour of single, multi-arch and open-sprandel arch masonry bridges. *Arch'01. 3rd int. arch bridges conf*. p. 523-530. Paris.

Prentice, D.J., Ponniah, D.A. 1994. Testing of multi-span model masonry arch bridges. *Proc. centenary year bridge conference*, Cardiff, Elsevier Science, pp. 169-174.